

Polarization Conductivity in *p*-Type Germanium\*†

STUART GOLIN‡

*Department of Physics and Institute for the Study of Metals, University of Chicago, Chicago, Illinois*

(Received 23 May 1963)

The ac conductivity  $\sigma_{ac}$  of *p*-type Ge was measured over the frequency range of  $10^3$  to  $10^5$  cps and in the impurity conduction temperature range of 1.2 to 4.2°K. Doping by transmutation insured a constant donor to acceptor concentration ratio of 0.4. The acceptor concentration ranged from  $3 \times 10^{14}$  to  $2 \times 10^{15}$ /cc. The observed frequency and concentration dependence of  $\sigma_{pol} = \sigma_{ac} - \sigma_{dc}$  can be understood on the basis of the polarization model of Pollak and Geballe. The observed temperature dependence can be understood by considering the interaction between ionized donors and electrons. From the absolute magnitude of  $\sigma_{pol}$ , the Bohr radius of the acceptor wave function is found to be about 74 Å, in good agreement with that found from dc measurements.

## I. INTRODUCTION

IMPURITY conduction has been studied extensively<sup>1</sup> since its discovery in SiC in<sup>2</sup> 1946 and in Ge in 1950.<sup>3</sup> At low-impurity concentrations this conduction process results from charge exchange between neighboring majority impurity sites due to a small overlap of the localized wave functions of the individual majority impurity centers. Since charge is transferred only from occupied to unoccupied majority centers, charge exchange requires compensating minority impurities. The fractional number of majority impurities which are ionized at  $T=0^\circ\text{K}$  is the compensation ratio  $K$ ; it is the ratio of minority to majority impurity concentrations. The conductivity due to this process is very small and can be observed only at low temperatures when there are a negligible number of carriers in the conduction and valence bands.

Consider, in particular, a compensated *p*-type semiconductor. Impurities are ionized as the donor electrons go into the lower lying acceptor states. The charged impurities set up random fields in the crystal which cause local fluctuations in the energy levels of the acceptors. These energy differences impede the motion of the electrons as they drift through the crystal from acceptor to acceptor under an applied dc electric field. This gives rise to the observed temperature dependence of impurity conduction.<sup>4</sup>

The ease with which an electron tunnels between two acceptors depends on the distance as well as the energy separating them. Both the spatial and energy separation of adjacent acceptors in the path of the electron vary from point to point in the crystal because the impurities occupy random lattice sites. The statistics of following an electron through such a crystal is very complicated.

Hence, dc measurements offer no direct measure of the tunneling process between individual acceptor pairs.

However, even if an electron is confined to two acceptors and cannot support a dc current, it will contribute to an ac current. The average fraction of time it spends on each acceptor will depend on the energy difference of the two states. An applied ac field will alter this energy difference and produce a net polarization which will lag behind the field because the tunneling (transition) rates are finite. In general, the part of the polarization which is out of phase with the field is measured as a dielectric loss or an ac conductivity. We will call it the polarization conductivity  $\sigma_{pol}$ . Similarly, the in-phase part of the polarization makes a contribution to the dielectric constant which we will call the polarization dielectric constant  $\epsilon_{pol}$ .

Pollak and Geballe<sup>5</sup> (PG) observed in *n*-type silicon that the ac conductivity  $\sigma_{ac}$  is larger than the dc conductivity  $\sigma_{dc}$ . They attributed this difference to the polarization conductivity. Thus,

$$\sigma_{pol} = \sigma_{ac} - \sigma_{dc}. \quad (1)$$

(In their notation  $\sigma_{ac} = \sigma - \sigma_{dc}$ .) Similarly,

$$\epsilon_{pol} = \epsilon_{ac} - \epsilon_{Ge}. \quad (2)$$

PG assumed that the only contribution to the polarization conductivity comes from pairs; i.e., from electrons which are confined to only two acceptors. They constructed a model which accounts well for the frequency dependence of  $\sigma_{pol}$ , but not for the temperature dependence. This made it difficult to compare the concentration dependence and absolute magnitude of  $\sigma_{pol}$  with theory.

The measurements reported here were made to test the applicability of the model of PG to germanium. Germanium has the advantage that it can be doped by thermal neutron irradiation to produce *p*-type samples.<sup>6</sup> The compensation ratio  $K$ , which is very important in impurity conduction,<sup>7</sup> is  $K=0.4$  for all samples so produced. Another advantage of doping by irradiation

\* Submitted as a thesis in partial fulfillment of the requirements for the degree of Doctor of Philosophy at the University of Chicago.

† Supported by the U. S. Air Force Office of Scientific Research through grant number AFOSR62-178.

‡ National Science Foundation Predoctoral Fellow.

<sup>1</sup> For references see N. F. Mott and W. D. Twose, *Suppl. Phil. Mag.* **10**, 107 (1961).

<sup>2</sup> G. Busch and H. Labhart, *Helv. Phys. Acta* **19**, 463 (1946).

<sup>3</sup> C. S. Hung and J. R. Gliessman, *Phys. Rev.* **79**, 726 (1950).

<sup>4</sup> N. F. Mott, *Can. J. Phys.* **34**, 1356 (1956).

<sup>5</sup> M. Pollak and T. H. Geballe, *Phys. Rev.* **122**, 1742 (1961).

<sup>6</sup> J. W. Cleland, K. Lark-Horovitz, and J. C. Pigg, *Phys. Rev.* **78**, 814 (1950).

<sup>7</sup> H. Fritzsche and M. Cuevas, *Phys. Rev.* **119**, 1238 (1960).

is the guarantee that the impurities will be located at random. This method of doping is less useful in silicon because of the difficulty of annealing out the radiation damage.

## II. EXPERIMENTAL PROCEDURE

The polarization conductivity  $\sigma_{pol} = \sigma_{ac} - \sigma_{dc}$  can be meaningfully measured only when  $\sigma_{dc}/\sigma_{pol} < 1$  (i.e.,  $\sigma_{dc} < \frac{1}{2}\sigma_{ac}$ ). This fact limits the temperature, frequency, and impurity concentration range available for measurement. In Fig. 1,  $\sigma_{dc}/\sigma_{pol}$  is plotted against concentration for  $10^3$  and  $10^5$  cps at 1.5 and 4°K. For fixed frequency, this ratio increases rapidly with concentration and temperature because  $\sigma_{dc}$  increases more rapidly than  $\sigma_{pol}$  with these quantities. The dc conductivity  $\sigma_{dc}$  increases even more rapidly with temperature above about 4°K as one leaves the impurity conduction range and holes are ionized into the valence band (in *p*-type germanium). For fixed temperature and impurity concentration,  $\sigma_{dc}/\sigma_{pol}$  decreases rapidly with increasing angular frequency  $\omega$ , since, as found also in silicon,<sup>5</sup>  $\sigma_{pol} \propto \omega^7$  in germanium.

The measurements were made in decade steps from  $10^2$  to  $10^5$  cps, and between 1.2 and 4.2°K. This restricted the acceptor concentration to less than  $10^{15}/cc$ . In silicon these measurements can be made up to about 20°K because of the higher ionization energies involved.

In general,  $\sigma_{ac}$  is very small so it is feasible to treat the sample as a dielectric and calculate  $\sigma_{ac}$  from the dielectric loss. Thus, the samples were cut into disks and placed between the electrodes of a capacitance cell as shown in Fig. 2. The dielectric loss was measured with a capacitance bridge. At the same time, the dc conductivity was measured with a vibrating reed electrometer.

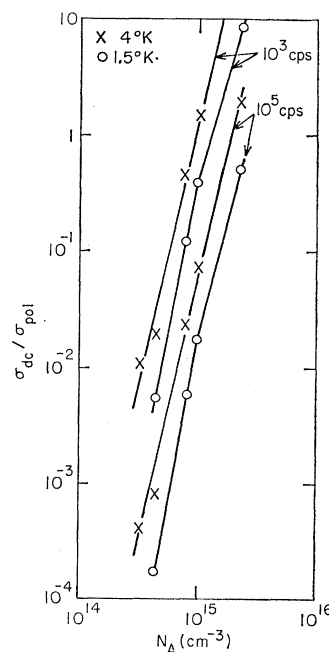
The temperature was measured with 0.1 W Allen Bradley carbon resistor which was calibrated against the vapor pressure of helium using a vapor pressure bulb.

### A. Bridge and Sample Holder

The ac measurements were made with a precision Schering capacitance bridge.<sup>8</sup> The bridge was used in the substitution mode, which means that readings are taken with the sample once connected and once disconnected at the bridge terminals. In the direct method, where measurements are made only with the sample connected, the values of capacitance and loss depend on all circuit elements in the bridge and, therefore, are subject to all of their errors. But in the substitution method, the errors in those circuit elements which are unchanged are largely eliminated. This is especially important when the sample has a low loss; i.e., low conductivity.

The quantities  $\sigma_{ac}$  and  $\epsilon_{pol}$  were calculated from the exact equations of bridge balance.<sup>9</sup> To test these equa-

FIG. 1. Concentration dependence of  $\sigma_{dc}/\sigma_{pol}$  at  $10^3$  and  $10^5$  cps at 4 and 1.5°K.



tions, impedances were formed from series and parallel combinations of known carbon resistors and high quality capacitors. The measured conductance agreed with the calculated value to within 2% over the range of the bridge in which most of the actual sample measurements were made.

A sensitive detector for the bridge was required as in some cases the onset of the nonohmic range of the sample was as low as 1 V/cm. This should be contrasted with silicon which can tolerate fields of hundreds of V/cm. The detector consisted of two amplifiers, an adjustable filter, and an oscilloscope. This proved adequate in most cases to realize the full accuracy of the bridge.

The sample holder sketched in Fig. 2 is a capacitance cell. It is designed to exclude liquid helium in order to avoid a change in the capacitance due to the changing

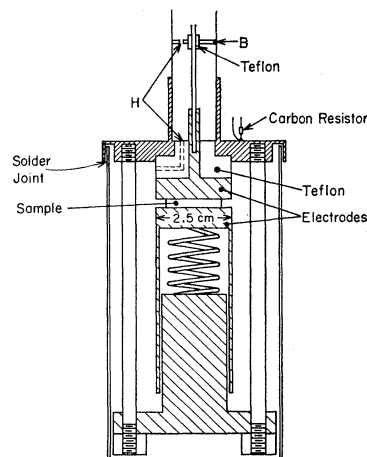


FIG. 2. Sample holder. H: hole to permit evacuation of cell. B: brass spacer and radiation shield.

<sup>8</sup> The General Radio 716-C.

<sup>9</sup> See Appendix A.

TABLE I. Sample characteristics.

Sample	Hall coefficient ( $\text{cm}^3 \text{C}^{-1}$ )		$N_A - N_D$ ( $\times 10^{14} \text{cm}^{-3}$ )	$N_A$ ( $\times 10^{14} \text{cm}^{-3}$ )
	300°K	77°K		
A	38 400	32 200	1.94	3.2
B	29 900	24 400	2.56	4.3
C	16 700	13 300	4.7	7.8
D	12 800	10 900	5.7	9.5
E	5 840	4 890	12.8	21.4

helium level and fluctuations due to the boiling of the liquid. About 1-cm Hg of helium at room temperature was admitted to the cell as a heat exchange gas.

To minimize the capacitance and conductance in parallel with the sample, we used rigid coaxial leads with an air (or He gas) dielectric and Teflon spacers for the center lead.

### B. Samples

Pure single crystals, whose top and bottom room-temperature resistivities exceeded 50 and 7  $\Omega\text{-cm}$ , respectively, were irradiated by thermal neutrons<sup>10</sup> for different lengths of time. Following neutron absorption, different isotopes of germanium decay into gallium, arsenic, and selenium, respectively. Gallium predominates and *p*-type Ge results after the decay is complete. The crystals were annealed about eight months after irradiation.<sup>11</sup>

The Hall coefficient was measured at room temperature and 77°K and the lower value was used to calculate  $N_A - N_D$ .  $N_A$  and  $N_D$  are the acceptor and donor concentrations, respectively. Since each selenium donor is doubly ionized and compensates two acceptors, it is counted here as two donors.  $N_A - N_D$  may be underestimated by about 10% because the magnetic field used (about 7000 G) is not in the high-field limit.<sup>7</sup> The results are given in Table I. The compensation ratio  $K$  may not be exactly the same for all samples due to impurities in the samples before irradiation. This is most serious for sample A which received the smallest radiation dose. From the Hall coefficient of the starting material, we estimate that  $K$  deviates from 0.4 by less than 3% for this sample.

The samples were cut into discs about 2-mm thick and  $1\frac{1}{2}$  cm in diameter. It was necessary to etch them to eliminate edge conduction which otherwise would short out the sample. The flat surfaces were lapped or sandblasted and then electroplated with gold or rhodium. A lower impedance contact was obtained when the surface was sandblasted rather than lapped before electroplating, but it made little difference whether gold or rhodium was used. Figure 4 illustrates the effect of surface treatment on  $\sigma_{\text{pol}}$  for sample B. The discrepancy

<sup>10</sup> They were irradiated in the CP-5 reactor of the Argonne National Laboratory.

<sup>11</sup> See Ref. 7 for details about the irradiation and annealing procedures.

for different surface treatments and for different thicknesses are of the order of 10%. For samples 2-mm thick, both the ac and dc contact impedances are estimated to be of the order of 10% of the bulk ac and dc impedances, respectively.

To test for edge conduction and other spurious effects, measurements were made on a pure specimen of germanium whose room temperature resistivity is 54  $\Omega\text{-cm}$ . At 4°K the conductance at each frequency was at least an order of magnitude below that of sample A, the least conductive of our samples, over the measured temperature range.

### C. Effect of Light

Light can appreciably increase the conductivity of germanium in the impurity conduction region by exciting carriers into the valence and conduction bands. Even room temperature radiation can cause significant errors because the ionization energy of the acceptors is only about 0.01 eV. Great care was taken to protect the sample from light, especially from thermal radiation which originates at the top of the cryostat and goes down the coaxial leads.

Despite these precautions, photoconductivity was detected in sample A by comparing dc measurements taken in the ac apparatus with those taken in a "light-tight" sample holder. (The light-tight apparatus is not useful for ac measurements because of the large capacitance caused by the extra shielding.)

However, since valence band conduction should be frequency-independent except at very high frequencies, it is clear that there can be little error from light in  $\sigma_{\text{pol}}$  when  $\sigma_{\text{ac}} \gg \sigma_{\text{dc}}$ , since both ac and dc measurements were performed in the same ac apparatus. This condition applies to sample A over our frequency and temperature range. To estimate the effect of light on  $\sigma_{\text{pol}}$  for the other samples, we note that the photoconductivity should be proportional to  $N_A - N_D$ , the concentration of neutral acceptors. On the other hand, we find that  $\sigma_{\text{pol}}$  is approximately proportional to  $N_D(N_A - N_D)$ .<sup>12</sup> Therefore,  $\sigma_{\text{pol}}/\sigma_{\text{light}} \propto N_D$  is least for sample A which has the smallest donor concentration. Hence, we conclude that light has caused no significant error in  $\sigma_{\text{pol}}$ .

## III. RESULTS

In general, the polarization conductivity can be considered to be complex. Then  $\sigma_{\text{pol}}$  is the real part and  $\omega\epsilon_0\epsilon_{\text{pol}}$  is the imaginary part, where  $\epsilon_0$  is the permittivity of space. (mks units are used throughout.) These quantities are plotted in Fig. 3 for samples A and C at 1.2 and 4°K. As found in silicon,<sup>5</sup>  $\sigma_{\text{pol}}$  of germanium follows a power law

$$\sigma_{\text{pol}} \propto \omega^s, \quad (3)$$

where  $s \approx 0.7$ .

<sup>12</sup>  $\sigma_{\text{pol}}$  increases slightly more rapidly with concentration than  $\sigma_{\text{pol}}^L$ . The latter is plotted in Fig. 11.

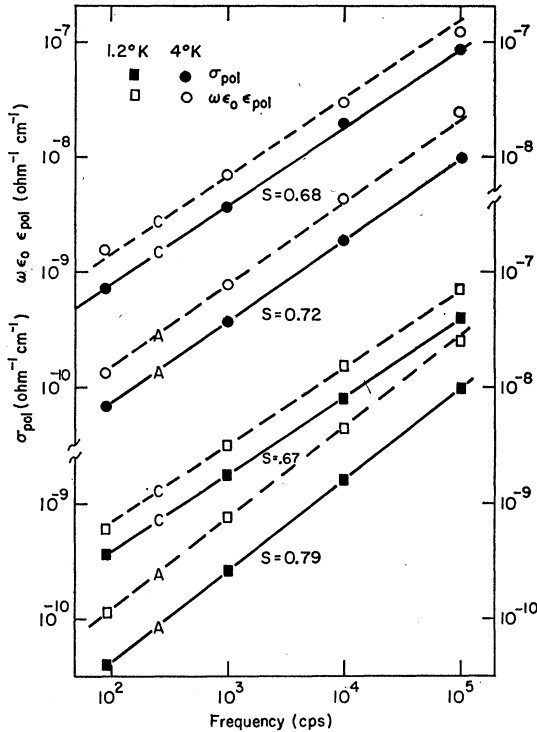


FIG. 3. The real and imaginary parts of the measured complex polarization conductivity,  $\sigma_{pol}$  and  $\omega\epsilon_0\epsilon_{pol}$ , respectively, are plotted against frequency at 1.2 and 4°K for samples A and C. The dashed lines are the theoretical curves for  $\omega\epsilon_0\epsilon_{pol}$  as calculated from  $\sigma_{pol}$  using Eq. (4).

The real and imaginary parts of the complex polarization conductivity are not independent of each other but are related through the Kramers-Kronig relations. These imply, for the power law dependence of Eq. (3),<sup>13</sup>

$$\omega\epsilon_0\epsilon_{pol} = \sigma_{pol} \tan \frac{1}{2}\pi S. \quad (4)$$

The applicability of Eqs. (3) and (4) is illustrated in Fig. 3. The dashed lines are the theoretical curves of  $\omega\epsilon_0\epsilon_{pol}$  as calculated from Eq. (4) and the measured values of  $\sigma_{pol}$  (actually the solid lines through them). The agreement between the theoretical curves of  $\omega\epsilon_0\epsilon_{pol}$  and the measured points is good. It demonstrates the validity of the measurements.<sup>14</sup> Since  $\sigma_{pol}$  and  $\epsilon_{pol}$  are not independent quantities, the discussion will be confined to  $\sigma_{pol}$ .

Figure 4 illustrates the temperature dependence of

<sup>13</sup> For our system, the Kramers-Kronig relations may be  $\epsilon_0\epsilon_{pol} = -(2/\pi) \int_0^\infty \sigma_{pol}(y) (\omega^2 - y^2)^{-1/2} dy$ , where the principle part of the integral is understood. [See, for example, J. R. Macdonald and M. K. Brachman, *Rev. Mod. Phys.* **28**, 393 (1956), Eq. (30).] This reduces to Eq. (4) when  $\sigma_{pol}(\omega) \propto \omega^S$ . [Bierens de Haan, *Nouvelles Tables D'Intégrales Définies* (G. E. Stechert and Company, New York, 1939), p. 43, Table 17, Eq. (11).]

<sup>14</sup> The Kramers-Kronig relations are used to determine  $C_0$ , the capacitance in parallel with the system of acceptor pairs (see Ref. 5 and Appendix A in the present paper). This does not materially weaken the assertion that Eq. (4) is obeyed since  $C_0$  is the only adjustable parameter and it is determined only at one temperature (1.2°K).

$\sigma_{pol}$  for the different samples. This dependence is stronger at higher impurity concentrations and at lower frequencies.

## IV. THEORY

### A. The Model

Consider an electron which is confined to a pair of acceptors and tunnels between them at a certain statistical rate. An applied dc electric field will polarize the pair in a time which is of the order of the tunneling time. The time derivative of this polarization is measured as a current. This is analogous to the response of a series RC circuit to a dc voltage. Here the current is given by the time derivative of the charge on the condenser. The real part of the ac conductance of the RC circuit is  $\omega^2\tau c / (1 + \omega^2\tau^2)$ , where  $\tau$  is the RC time constant. The conductance increases quadratically with frequency when  $\omega\tau \ll 1$  and saturates when  $\omega\tau \gg 1$ . The conductivity due to many noninteracting acceptor pairs will be a sum of terms of this form, each term with the  $\tau$  value of the pair it represents. Each term of the sum increases monotonically with frequency; hence, the total conductivity must increase monotonically with frequency.

The basic assumption of the pair model of PG is that the polarization conductivity is due to electrons that tunnel back and forth between two acceptors and not among larger groups of acceptors. This is valid if each electron is localized on a pair of acceptors for a time long compared with the tunneling time between the two acceptors. The validity of this assumption of localization is discussed in Part C.

Since an electron can tunnel only from an ionized acceptor to a neutral one, a pair must be singly ionized to contribute to the polarization conductivity.

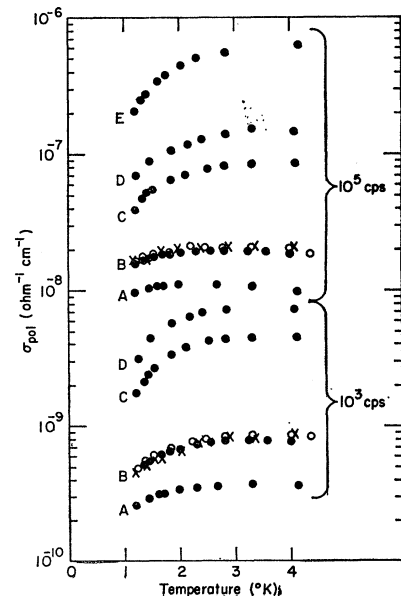


FIG. 4. For the various samples,  $\sigma_{pol}$  is plotted against  $T$  at  $10^3$  and  $10^5$  cps. Three different measurements are shown on two different slices from sample B to illustrate the effect of surface treatment: ●—1.1 mm thick, rhodium plated on a sandblasted surface. ○—1.9 mm thick, rhodium plated on a sandblasted surface. ×—1.9 mm thick, gold plated on a lapped surface.]

We now outline the model of PG using the terminology of a  $p$ -type semiconductor.

Consider a cube of unit volume containing one singly ionized acceptor pair. Denote the acceptors by 1 and 2. Let  $\Delta$  and  $r$  be the energy and distance separating them, and let  $\theta$  be the angle between the line joining the acceptors and the applied field. ( $\Delta$  and  $r$  will be referred to as the energy and size of the pair, respectively.)

The current in the field direction is given by

$$j(t) = \dot{p}, \quad (5)$$

where (taking acceptor 2 as the origin)

$$\dot{p} = er \cos\theta f_1. \quad (6)$$

The probability  $f_1$  that the electron is on acceptor 1 is given by the solution of

$$f_1 + f_2 = 1, \quad (7)$$

$$\dot{f}_1 = W_{21}f_2 - W_{12}f_1, \quad (8)$$

where  $W_{12}$  and  $W_{21}$  are the transition rates.

The response of this system to a dc electric field  $\mathcal{E}$  which is turned on at  $t=0$  is

$$f_1(t) = f_1(\infty) + [f_1(0) - f_1(\infty)]e^{-t/\tau}, \quad (9)$$

where

$$\tau = (W_{12} + W_{21})^{-1} \quad (10)$$

is the relaxation time of the pair.

The difference,  $f_1(0) - f_1(\infty)$ , is determined from Boltzmann statistics from  $\Delta$  and the change in  $\Delta$  due to  $\mathcal{E}$ . In the limit of small  $\mathcal{E}$

$$f_1(0) - f_1(\infty) = \frac{er \cos\theta}{4kT \cosh^2(\Delta/2kT)} \mathcal{E}. \quad (11)$$

The current  $j(t)$  follows from Eqs. (5), (6), (9), and (11). The frequency response of the pair is given by

$$\frac{j(\omega)}{\mathcal{E}(\omega)} = \frac{e^2 r^2 \cos^2\theta}{4kT \cosh^2(\Delta/2kT)} \frac{\omega^2 \tau}{1 + \omega^2 \tau^2}, \quad (12)$$

where  $j(\omega)$  and  $\mathcal{E}(\omega)$  are the Fourier transforms of  $j(t)$  and  $\mathcal{E}$ , respectively.

In generalizing to the physical situation of many pairs in the unit volume, PG assume that there is no interaction between pairs; i.e., that the field acting on a pair is the applied field, unaffected by the field produced by the polarization of the other active (singly ionized) pairs. Then the total conductivity is a sum of contributions from all active pairs. This assumption is valid in Si where the conductivity and, hence, the polarization in the crystal is very small. Even in Ge, where the assumption is not valid, the local conductivity (the conductivity in terms of the local field) is additive. This follows from the fact that the total polarization of the crystal must be a sum of the polarizations of each of the pairs (assuming that only pairs are impor-

tant). The local conductivity of a pair is proportional to its polarization divided by the local field acting on it. Also, on the average, the local field is the same for all active pairs [Eqs. (26) and (27)]. Hence, the local conductivity is additive.

The present calculation gives the local conductivity and this will be designated with the superscript  $L$ . The calculation of the local conductivity in terms of the measured conductivity is discussed in Part B.

Then, after integrating Eq. (12) over  $\theta$ , the local conductivity is given by

$$\sigma_{\text{pol}}^L = \frac{e^2 \omega}{12kT} \iint \frac{r^2 dp(r, \Delta)}{(\omega\tau + 1/\omega\tau) \cosh^2(\Delta/2kT)}, \quad (13)$$

where  $dp(r, \Delta)$  gives the density of singly ionized acceptor pairs of size  $r$  and energy  $\Delta$ .

Since  $dp(r, \Delta)$  is unknown, the integral cannot be evaluated in the general case. Therefore, PG just considered the high-temperature case and reduced the double integral over  $r$  and  $\Delta$  to a single integral over  $r$  which can be evaluated. This gives the correct frequency dependence of  $\sigma_{\text{pol}}^L$  but not the correct temperature dependence over the accessible temperature range. Unfortunately, valence band conduction (conduction band conduction in their case) becomes important before the high-temperature region is reached. However, to a good approximation, the double integral can be replaced by two single integrals, giving us some insight into the temperature dependence.

We write  $dp(r, \Delta) = H(\Delta, r) d\Delta N(r) dr$ , where  $N(r)$  gives the concentration of singly ionized acceptor pairs of size  $r$ , and  $H(\Delta, r)$  gives the probability that the energy of such a pair is  $\Delta$ .

As will be seen shortly,  $\tau$  is an exponential function of  $r$  but is independent of  $\Delta$  to first order in  $\Delta/2kT$ . This strong dependence on  $r$  causes the term  $(\omega\tau + 1/\omega\tau)^{-1}$  in the integrand of Eq. (13) to behave as a  $\delta$  function. Equation (13) becomes

$$\sigma_{\text{pol}}^L = \frac{e^2 \omega}{12kT} \mathfrak{I}(T, r_{\text{max}}) \int_0^\infty \frac{r^2 N(r) dr}{\omega\tau + 1/\omega\tau}, \quad (14)$$

where

$$\mathfrak{I}(T, r_{\text{max}}) = \int_0^\infty H(\Delta, r_{\text{max}}) \cosh^{-2}(\Delta/2kT) d\Delta, \quad (15)$$

$r_{\text{max}}$  being defined as the value of  $r$  which maximizes the  $r$  integrand.

Because of the peaked nature of the  $r$  integrand (Fig. 6), the major contribution to  $\sigma_{\text{pol}}^L$  comes from pairs whose size is near  $r_{\text{max}}$ . For these pairs  $\omega\tau \approx 1$ .<sup>15</sup> Since  $\tau$  increases exponentially with  $r$ ,  $r_{\text{max}}$  decreases slowly with frequency (Fig. 7). (This is to be expected since reducing the distance between two acceptors will

<sup>15</sup> Because of the small but finite influence of its numerator, the  $r$  integrand (Eq. 14) is maximum when  $\omega\tau > 1$  rather than  $\omega\tau = 1$  (Fig. 6).

increase the frequency with which an electron can tunnel between them.) Thus, ac measurements are very selective as to pair size and this pair size decreases with frequency.

If the acceptors are ionized at random,  $N(r)$  is given by

$$N(r)dr = 4\pi r^2 dr N_D(N_A - N_D). \quad (16)$$

Note that an acceptor pair is counted even if there is a third acceptor in between them. Such a triplet would also contribute to the conductivity so, unless triplets are treated explicitly, the above form for  $N(r)$  is perhaps the best approximation.

The ground-state acceptor wave function  $\psi$  is quite complicated but probably can be represented for our purpose by a weighted sum of an outer spherical one  $\psi^O$  and an inner one  $\psi^I$  which is unimportant for tunneling processes. Then

$$\psi = \beta\psi^O + (1 - \beta^2)^{1/2}\psi^I, \quad (17)$$

where  $\beta$  is unknown and will be assumed to be unity. Using the transition rates of Miller and Abrahams,<sup>16</sup> one finds

$$\tau = (b/T)(a/r)^2 e^{2r/a}, \quad (18)$$

where

$$b = \frac{T 9\pi\rho_0 S^5 \hbar^4 \epsilon_{Ge}^2 a^2}{\beta^2 4E_1^2 e^4} \times \frac{\tanh(\Delta/2kT)}{\Delta} \approx \frac{9 \times 10^{-14} T}{\Delta(mV)} \tanh(\Delta/2kT), \quad (19)$$

and where  $\rho_0$ =density of Ge=5.36 g/cc;  $S$ =speed longitudinal sound  $\approx 5.4 \times 10^5$  cm/sec;  $E_1$ =deformation potential  $\approx 4$  eV;  $\epsilon_{Ge}$ =dielectric constant of germanium =16;  $a$ =Bohr radius of the acceptor wave function  $\approx 74.5$  Å. This value was chosen to give the best absolute magnitude agreement with experiment (Sec. V.A).

Because of the  $\cosh^2$  term in Eq. (15), only pairs with  $\Delta < 2kT$  make an appreciable contribution to  $\sigma_{pol}^L$ . Expanding the hyperbolic tangent in Eq. (19),

$$b \approx \frac{9 \times 10^{-14}}{2k} \left[ 1 - \frac{1}{3} \left( \frac{\Delta}{2kT} \right)^2 + \dots \right] \approx 5 \times 10^{-13} \text{ }^\circ\text{K sec.} \quad (20)$$

Hence, to first order in  $\Delta/2kT$ ,  $\tau$  is independent of  $\Delta$ .

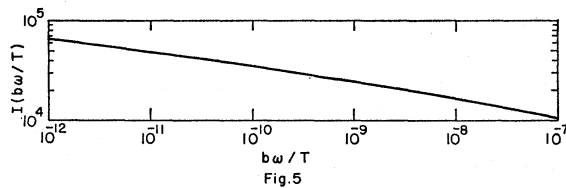


FIG. 5. Plot of the spatial integral as defined in Eq. (22).

<sup>16</sup> A. Miller and E. Abrahams, Phys. Rev. **120**, 745 (1960).

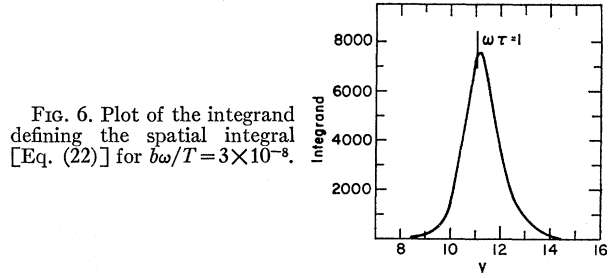


FIG. 6. Plot of the integrand defining the spatial integral [Eq. (22)] for  $b\omega/T = 3 \times 10^{-8}$ .

From Eqs. (16) and (18), Eq. (14) becomes

$$\sigma_{pol}^L = \frac{\pi e^2 N_D (N_A - N_D)}{3kT} a^5 \omega I(b\omega/T) \mathcal{C}(T, r_{max}), \quad (21)$$

where

$$I(b\omega/T) = \int_0^\infty \frac{y^4 dy}{(e^{2y} y^{-2} b\omega/T) + (e^{2y} y^{-2} b\omega/T)^{-1}} \quad (22)$$

(and  $y=r/a$ ).  $I(b\omega/T)$  was evaluated numerically and is plotted in Fig. 5. To illustrate its peaked nature, the integrand defining  $I(b\omega/T)$  is plotted in Fig. 6 for  $b\omega/T = 3 \times 10^{-8}$ , corresponding to a frequency of  $10^4$  cps and a temperature  $\approx 1^\circ\text{K}$ . Here  $y_{max} = r_{max}/a = 11.2$ . In general,  $y_{max}$  is given by the solution of

$$b\omega/T = y_{max}^2 \exp(-2y_{max}) \times [(y_{max} + 1)/(y_{max} - 3)]^{1/2}. \quad (23)$$

This is plotted in Fig. 7.

From the above,  $b$  is to be evaluated at  $\Delta=0$ . Perhaps it would be a better approximation to evaluate  $b$  at  $\Delta = \Delta_{av}$ , where  $\Delta_{av}$  is defined by

$$\int_0^{\Delta_{av}} H(\Delta, r_{max}) \cosh^{-2}(\Delta/2kT) d\Delta = \frac{1}{2} \mathcal{C}(T, r_{max}). \quad (24)$$

In this case  $\mathcal{C}(T, r_{max})$  and the  $r$  integrand are coupled in that each must be evaluated to determine a parameter in the other. This is not serious, as an iteration procedure converges rapidly. However, the change in  $\sigma_{pol}^L$  by this refinement is small because  $I(b\omega/T)$  is a weak

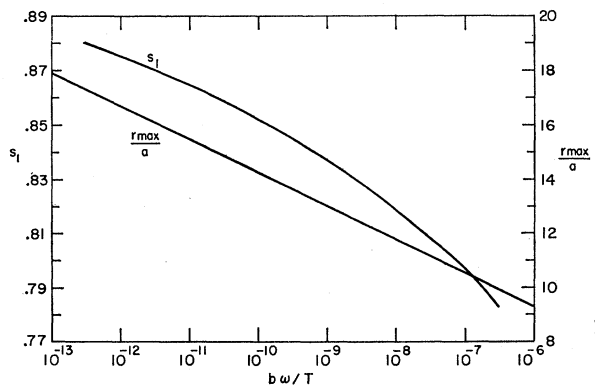


FIG. 7. Plot of  $r_{max}/a$  (see text) and  $s_1$  [Eq. (39)] versus  $b\omega/T$ .

function of its argument (Fig. 5) and because  $b$  is a weak function of  $\Delta/2kT$ . The extent of the effect depends on the form of  $H(\Delta, r_{\max})$ ; it is less than 3% for the cases considered in Sec. V.A. Hence, we use the simpler procedure of defining  $b$  at  $\Delta=0$ .

### B. Local Field

To compare theory with experiment, we must be able to calculate  $\sigma_{\text{pol}}^L$  from measurable quantities. We have

$$j^* = \sigma_{\text{pol}}^* \mathcal{E}_{\text{applied}}^* = \sigma_{\text{pol}}^* L \mathcal{E}^{*L}, \quad (25)$$

where the asterisk signifies a complex quantity. It can be shown that, when the electrons are localized,<sup>17</sup>

$$\mathcal{E}^{*L} = \alpha^* \mathcal{E}_{\text{applied}}^*, \quad (26)$$

where

$$\alpha^* = 1 + \epsilon_{\text{pol}}^*/3\epsilon_{\text{Ge}}. \quad (27)$$

Then

$$\sigma_{\text{pol}}^{*L} = \sigma_{\text{pol}}^*/\alpha^*. \quad (28)$$

This form for  $\alpha^*$  can be made plausible. From the theory of dielectrics it is known that the field at an atomic center is larger than the applied field by the factor  $\alpha^* = 1 + \frac{1}{3}(\epsilon_{\text{ac}}^* - \epsilon_s)$ , where  $\epsilon_{\text{ac}}$  is the dielectric constant of the material and  $\epsilon_s$  is that of space, i.e., unity. Consider a crystal of Ge in which are two acceptors some 1000 Å apart. (This is a typical value of  $r_{\max}$ .) Surely they will see the applied field and not the local field at the center of a germanium atom. Thus, the dielectric constant of pure Ge does not directly affect the "local" field at the center of an active pair. To account for this fact in the expression for  $\alpha^*$ ,  $\epsilon_s$  must be taken as the dielectric constant of pure Ge,  $\epsilon_{\text{Ge}}$ .

The dielectric constant of germanium is important, however, in that it reduces the interaction between active pairs. The term  $\frac{1}{3}(\epsilon_{\text{ac}}^* - \epsilon_{\text{Ge}})$  represents this interaction and thus must be reduced by the factor  $\epsilon_{\text{Ge}}$ . Hence, Eq. (27).

An alteration in Eq. (27) is required because the electrons are not completely localized as has been assumed. In fact, when the electrons are completely free, the local and applied fields are equal and  $\alpha^* = 1$ . A measure of the localization is  $\sigma_{\text{pol}}/\sigma_{\text{ac}}$ : When  $\sigma_{\text{pol}}/\sigma_{\text{ac}} = 1$ ,  $\sigma_{\text{dc}} = 0$  and the electrons are completely localized; when  $\sigma_{\text{pol}}/\sigma_{\text{ac}} = 0$ ,  $\sigma_{\text{dc}} \gg \sigma_{\text{pol}}$  and the electrons are free. Exactly how  $\alpha^*$  should depend on  $\sigma_{\text{pol}}/\sigma_{\text{ac}}$  is not known; the simplest form which is correct in the limiting cases of  $\sigma_{\text{pol}}/\sigma_{\text{ac}} = 0$  and 1 is

$$\alpha^* = 1 + (\sigma_{\text{pol}}/\sigma_{\text{ac}})(\epsilon_{\text{pol}}^*/3\epsilon_{\text{Ge}}). \quad (29)$$

<sup>17</sup> This results from the Lorentz field of the charge on the surface of a uniformly polarized sphere centered about the pair under consideration. It is assumed that the field produced by all of the other dipoles within the sphere is zero at the central dipole. This is true on the average under the assumptions that (1) the dipoles are points; (2) they are located at random; (3) the polarization of any other dipole in the sphere is independent of its location relative to the central dipole. The dipoles may differ in strength and orientation.

TABLE II. Comparison of  $R_A$  (the average distance between acceptors) and  $r_{\max}$  at  $T=1.5^\circ\text{K}$ .

$\omega/2\pi$ (cps)	$r_{\max}/a$	$r_{\max}$ (Å)	Sample	$R_A = (\frac{1}{3}\pi N_A)^{-1/3}$ (Å)
$10^2$	13.8	1030	A	900
$10^3$	12.6	940	B	810
$10^4$	11.3	840	C	670
$10^5$	10.1	750	D	620
			E	470

Putting Eq. (29) into Eq. (28) and taking the real parts of both sides, we find

$$\sigma_{\text{pol}}^L = \sigma_{\text{pol}} / \left[ \left( 1 + \frac{\sigma_{\text{pol}} \epsilon_{\text{pol}}}{\sigma_{\text{ac}} 3\epsilon_{\text{Ge}}} \right)^2 + \left( \frac{\sigma_{\text{pol}}}{\sigma_{\text{ac}}} \frac{\sigma_{\text{pol}}}{3\omega\epsilon_0\epsilon_{\text{Ge}}} \right)^2 \right]. \quad (30)$$

The ratio  $\sigma_{\text{pol}}/\sigma_{\text{pol}}^L$  varies from 1.0 to 1.5 for the present data. It increases with impurity concentration and decreases with frequency.

### C. Localization Assumptions

There are three assumptions of "localization." (1) The acceptor concentration must be sufficiently low that the acceptor states are localized and interact only weakly with each other. This requires  $R_A/a > 5$ , where  $R_A$  is the average distance between acceptors. This condition applies to all of the samples reported here. ( $R_A$  is tabulated in Table II.  $a \approx 74$  Å.)

(2) The pair model assumes that the ground states of the acceptors of a pair are localized and interact only weakly with each other. This holds when the overlap of the two wave functions is small, i.e., when  $r/a > 5$ . Since for fixed frequency, only those pairs of size  $r_{\max}$  are important, this requirement becomes  $r_{\max}/a > 5$ . Table II demonstrates that this condition applies to our frequency range.

(3) The pair model requires an electron to be confined to an active pair for times long compared to the tunneling time. This is the case when the distance from the pair to the nearest (third) acceptor is larger than the size of the pair because the tunneling rate decreases exponentially with distance. Since for fixed frequency only those pairs of size  $r_{\max}$  are important, the electrons can be considered localized on pairs when  $r_{\max} < R_A$ . This situation is borderline (Table II) and deviations from the pair model are to be expected. However, as the temperature is lowered, the electrons become less mobile. Hence, the validity of the pair model should improve with decreasing temperature.

Henceforth, the question of localization will refer only to the third, most restrictive, assumption. [The three assumptions are not independent of each other; if (2) and (3) apply, (1) must also apply.]

The pair model breaks down when the electrons are no longer localized on acceptor pairs and multiple-tunneling processes become important. In the first

stage of this breakdown, the electrons will still be confined to groups of three or more acceptors. Consider a group of acceptors which is polarized by a dc field in a time  $\tau$ . (This is an oversimplification because a single relaxation time cannot adequately describe the response of a group of more than two acceptors to an applied field.) The net dipole moment of this group will, in general, be larger than that of a pair with the same  $\tau$ , since a larger dipole moment can be produced in a given time by multiple transitions than by a single transition. Since, for fixed  $\tau$ , the contribution to the ac conductivity of a pair (or other polar system) is proportional to the square of the dipole moment [Eq. (12)], we expect groups to make a larger contribution to the ac conductivity than the pairs they replace.

Since the importance of groups increases with concentration (for fixed frequency and temperature), we would expect the concentration dependence of  $\sigma_{\text{pol}}^L$  to exceed that predicted by the pair model. Similarly, the frequency dependence  $s$  [Eq. (3)] should be smaller than the theoretical, and should decrease with concentration. Because multiple transitions become more frequent as  $T$  is increased from 0°K,  $s$  should decrease with temperature. These deviations from the pair model are observed experimentally (Sec. V).

## V. COMPARISON WITH EXPERIMENT

### A. Temperature Dependence and Absolute Magnitude

The absolute magnitude of the polarization conductivity varies as the fifth power of the Bohr radius  $a$  [Eq. (21)] of the acceptor wave function, and is a relatively insensitive function of the other parameters. Unfortunately, the value of  $a$  is in doubt. Kohn and Schechter<sup>18</sup> have calculated a value of 43 Å by a variational method. Fritzsche and Cuevas,<sup>7</sup> in fitting their data on dc measurements with Miller and Abrahams' theory,<sup>16</sup> obtained  $a=90$  Å. This last value is somewhat uncertain due to very complicated averaging procedures required in the dc theory. Miller<sup>19</sup> then made further variational calculations which confirmed Fritzsche and Cuevas' result. Because of the uncertainty in  $a$ , it will be treated as a parameter.

The temperature dependence of the polarization conductivity is given by [Eq. (21)]

$$\sigma_{\text{pol}}^L \propto T^{-1} I(b\omega/T) \mathcal{C}(T, r_{\text{max}}). \quad (32)$$

Unfortunately,  $\mathcal{C}(T, r_{\text{max}})$  cannot be evaluated as  $H(\Delta, r_{\text{max}})$  is unknown.  $H(\Delta, r_{\text{max}})$  is calculated in Appendix B on the assumptions<sup>20</sup>: (1) The nearest acceptor to each donor is ionized by that donor and forms one member of an active (singly ionized) pair; (2) The energy  $\Delta$  of the pair is caused only by the donor

<sup>18</sup> W. Kohn and D. Schechter, Phys. Rev. **99**, 1903 (1955).

<sup>19</sup> A. Miller (unpublished).

<sup>20</sup> This approach was suggested by M. Pollak (to be published).

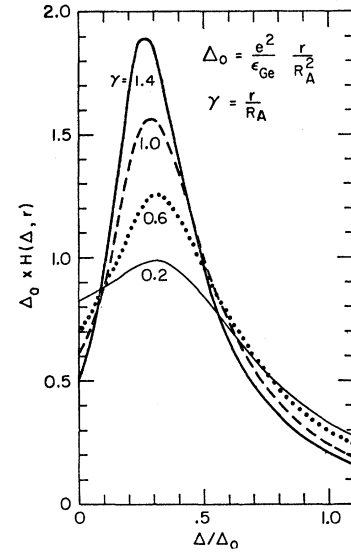


FIG. 8. Plot of  $\Delta_0 \times H(\Delta, r)$  versus  $\Delta/\Delta_0$  with  $\gamma = r/R_A$  as a parameter. See text for explanation.

which ionized it. These conditions are best met at low  $T$  and  $K$ , and they cannot be expected to yield quantitative agreement with our data.

The results of this calculation are plotted in Fig. 8. The relevant parameters are

$$\gamma = r/R_A, \quad (33)$$

$$\Delta_0 = e^2 r / \epsilon_{\text{Ge}} R_A^2, \quad (34)$$

where  $R_A = (\frac{4}{3}\pi N_A)^{-1/3}$  is the average distance between acceptors.

The product  $T\sigma_{\text{pol}}^L$  is plotted in Fig. 9 for  $10^4$  cps. Including the factor  $T$  emphasizes the role of  $\mathcal{C}$ , which is largely cancelled by the  $T^{-1}$  term in Eq. (32). [The temperature dependence of  $I(b\omega/T)$  is small.] The Bohr radius  $a$  was adjusted so that the theoretical curve for sample A agreed with experiment at 1.5°K. This yields

$$a = 74.5 \text{ \AA}. \quad (35)$$

Sample A is chosen as the standard since, as it has the

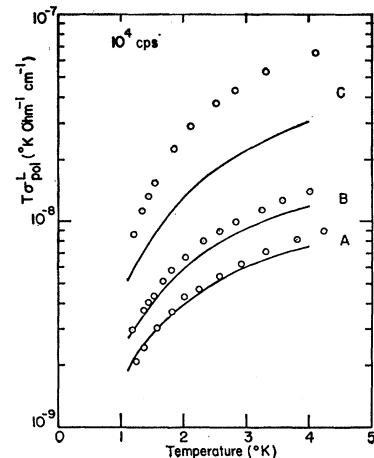


FIG. 9. Temperature dependence of  $T\sigma_{\text{pol}}^L$  for samples A, B, and C. The theoretical curves are based on  $H(\Delta, r)$  from Fig. 8 and on Eqs. (21) and (35).



lowest impurity concentration, the errors from non-localization should be the least for it (Sec. IV.C).

The agreement with experiment is good for samples A and B, but is poor for sample C, especially at the higher temperatures. Effects of nonlocalization (Sec. IV.C) are to be expected for sample C (see Table II). As anticipated in Sec. IV.C, these effects seem to be more pronounced at the higher temperatures where the potential barriers are unable to confine the electrons. Of course, deviations are still expected at higher temperatures since the assumptions on which  $H(\Delta, r_{\max})$  was calculated cease to apply. More convincing evidence of nonlocalization effects is given in parts B and C of this section.

The advantage in determining  $a$  in this way is that the effect of errors or uncertainties in other quantities is small because  $a$  appears as  $a^5$ . The least certain quantities,  $E_1$  and  $\beta$ , occur only in definition of  $b$  [Eq. (19)]. This is fortunate because  $b$  occurs only in the term  $I(b\omega/T)$  which is a slowly varying function of its argument (Fig. 5). The deformation potential  $E_1$  is uncertain to a factor of 2 since its weighted average over directions is unknown. The value of  $\beta$  [Eq. (17)] is uncertain and very difficult to calculate on theoretical grounds, but Miller<sup>19</sup> estimates it to be of the order of  $\frac{1}{2}$ . An underestimation of  $b$  by a factor of 10 would lead to an underestimation of  $a$  by only about 7% by this procedure.

There is further uncertainty in this value of  $a$  since the frequency dependence of  $\sigma_{\text{pol}}^L$  is not exactly as predicted. The measurements at  $10^6$  cps give a value of  $72 \text{ \AA}$  for  $a$ .

### B. Frequency Dependence

The frequency dependence of  $\sigma_{\text{pol}}^L$  is given by [Eq. (21)]

$$\sigma_{\text{pol}}^L \propto \omega I(b\omega/T) \mathcal{C}(T, r_{\max}). \quad (36)$$

The observed frequency dependence of  $\sigma_{\text{pol}}^L$  obeys a power law sufficiently closely to justify writing Eq. (36) as

$$\sigma \propto \omega^s, \quad (37)$$

where

$$s = s_1 + s_2, \quad (38)$$

$$s_1 = 1 + \frac{d \ln[I(b\omega/T)]}{d \ln \omega}, \quad (39)$$

$$s_2 = \frac{d}{d \ln \omega} \ln \mathcal{C}(T, r_{\max}). \quad (40)$$

Figure 7 shows  $s_1$  plotted against  $\omega b/T$ . It is independent of concentration. For our frequency range,  $s_1 \approx 0.8$ . It is a slowly varying function of its argument, increasing by about 0.01 with  $T$  over the measured temperature range and decreasing by about 0.02 as the frequency increases a decade. This variation is less than the experimental errors.

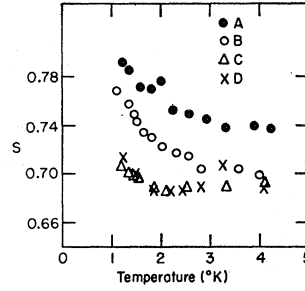


FIG. 10. Temperature dependence of  $s$  for samples A, B, C, and D.

In the high-temperature limit,  $s_2 = 0$ . This follows from the normalization of  $H(\Delta, r_{\max})$ :

$$\lim_{T \rightarrow \infty} \mathcal{C}(T, r_{\max}) = \int_0^{\infty} H(\Delta, r_{\max}) d\Delta = 1. \quad (41)$$

In the general case,  $\mathcal{C}(T, r_{\max})$  is very complicated and  $s_2$  has not been evaluated. However, we expect  $s_2$  to be positive and to increase with decreasing temperature. Decreasing the distance between two acceptors will, on the average, decrease the energy difference between them. Thus, by decreasing  $r_{\max}$ , increasing the frequency shifts  $H$  toward lower  $\Delta$  (see Fig. 8). Hence, because of the  $\cosh^2$  term in Eq. (15),  $\mathcal{C}$  increases with frequency. Therefore  $s_2 > 0$ . Lowering the temperature increases the effect of the  $\cosh^2$  term, and hence, increases  $s_2$ .

Similarly, increasing the impurity concentration will, on the average, increase the energy of a pair of given  $r_{\max}$ . Thus,  $s_2$  increases with concentration.

The average value of  $s$  over the frequency range is plotted in Fig. 10.  $s \approx 0.75$  in excellent qualitative agreement with the theory. Also, as expected from the discussion of  $s_2$ ,  $s$  decreases with temperature.

Quantitatively,  $s$  should never be below about 0.8. Yet, it is seen to be about 0.7 at 4°K. Also, contrary to the discussion of  $s_2$ ,  $s$  decreases with concentration. These discrepancies are probably due to the nonlocalization of electrons (Sec. IV.C).

Small discrepancies may also result from the form of the local field correction [Eq. (29)] being incorrect.

### C. Concentration Dependence

The theoretical concentration dependence of the polarization conductivity is [Eq. (21)]

$$\sigma_{\text{pol}}^L \propto N_D(N_A - N_D) \mathcal{C}(T, r_{\max}). \quad (42)$$

In the limit of high  $T$ , this reduces to [Eq. (41)]

$$\sigma_{\text{pol}}^L \propto N_D(N_A - N_D). \quad (43)$$

As the temperature is lowered, the concentration dependence is expected to fall. The argument is similar to the discussion of  $s_2$  in part B. Increasing the impurity concentration will, on the average, increase the energy of a pair of given  $r_{\max}$ . This causes  $\mathcal{C}(T, r_{\max})$  to decrease with concentration.

The temperature is "high" when it is higher than  $T_0 = \Delta_0/2k$ .  $T_0 \approx 6^\circ\text{K}$  for sample A at  $10^4$  cps, and is higher for the other samples. The high-temperature limit is never reached. Hence, we expect the concentration dependence to increase with temperature but to always be less than quadratic.

With frequency and temperature as parameters, the product  $T\sigma_{\text{pol}}L$  is plotted against  $N_D(N_A - N_D)$  in Fig. 11. (The factor  $T$  is included to separate curves of different temperatures.) The solid lines denote the quadratic dependence on concentration, and the dashed lines are drawn to connect points of one temperature where necessary for clarity. As expected, the concentration dependence increases with  $T$ . However, contrary to the theory, the experimental data rises slightly more rapidly than quadratic with concentration. This is particularly noticeable at  $4^\circ\text{K}$  between samples B and D. This suggests that the electrons are not completely localized (Sec. IV.C); i.e., that there are interactions of higher order than pairs which are important.

## VI. SUMMARY AND CONCLUSIONS

The ac conductivity of low-concentration *p*-type Ge samples was measured in the frequency range of  $10^2$  to  $10^5$  cps and in the temperature range of 1.2 to  $4.2^\circ\text{K}$ . This is the impurity-conduction-temperature range where charge is transported by tunneling from acceptor to acceptor. The frequency and concentration dependence of the polarization conductivity  $\sigma_{\text{pol}} = \sigma_{\text{ac}} - \sigma_{\text{dc}}$  can be understood on the basis of the pair polarization model of PG,<sup>5</sup> but deviations are observed suggesting that interactions of higher order than pairs are important in the polarization process. Allowance was made for the fact that a pair responds to the local and not the applied electric field. It was shown that the integration over all pairs can be replaced by the product of separate

integrals over the energy  $\Delta$  and size  $r$  of a pair, respectively. A calculation of the probability  $H(\Delta, r)$  that a singly ionized pair of size  $r$  will have an energy  $\Delta$  accounts qualitatively for the observed temperature dependence of the polarization conductivity. From the absolute magnitude of the polarization conductivity, the Bohr radius of the acceptor wave function was estimated to be about  $74 \text{ \AA}$ .

The selectivity to pair size may make ac measurements useful in the study of other transport phenomena involving impurity conduction. The validity of the pair model can be improved by extending the measurements to higher frequencies, keeping the concentration fixed. Similarly, by increasing the frequency, one can extend the concentration range for which the pair model applies. For a given concentration, the minimum frequency for which the pair model applies can be defined by  $r_{\text{max}} = R_A$ . This frequency follows from Fig. 7 or can be calculated from Eq. (23) by setting  $\nu_{\text{max}} = R_A/a$ .

## ACKNOWLEDGMENTS

The author wishes to express his gratitude to his research advisor, Professor H. Fritzsche, for suggesting this problem and for continued help and encouragement through all phases of the work. He is indebted to Professor Morrel H. Cohen for helping to clarify the calculation of the local field.

## APPENDIX A

The quantities  $\sigma_{\text{ac}}$  and  $\epsilon_{\text{pol}}$  are calculated from the exact equations of bridge balance. For the Schering bridge using the substitution method, the conductance  $G$  and capacitance  $C_b$  as seen by the bridge are given by

$$G = 2\pi F_0 \left( \frac{F}{F_0} \right)^2 \frac{C'(D-D')}{1 + (F/F_0)^2(D+D_0)^2}, \quad (44)$$

$$C_b = C' - C - \frac{(F/F_0)^2 C'(D-D')(D+D_0)}{1 + (F/F_0)^2(D+D_0)^2}, \quad (45)$$

where  $C$  is the capacitance of the standard capacitor and  $D$  is the reading of the dissipation factor dial.  $C'$  and  $D'$  are the corresponding quantities when the sample is disconnected (at the bridge terminals).  $F_0$  is the setting of the "range selector" switch and is chosen close to the applied frequency  $F$ .  $D_0 \approx 0.03$  for our bridge.<sup>8</sup>

These equations follow from the exact equations of balance<sup>21</sup> under two assumptions: (1) the insulation resistance of the standard capacitor is independent of the capacitance setting. This is valid since the standard capacitor has an air dielectric. (2) The dielectric loss of

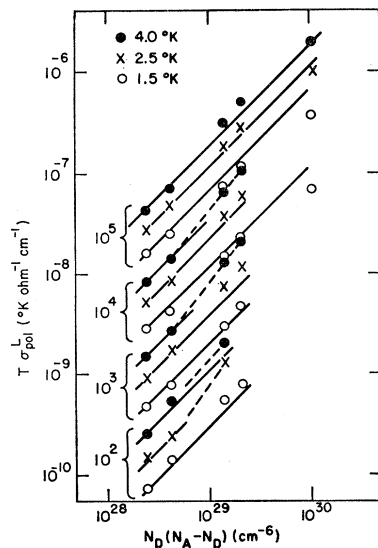


FIG. 11. Concentration dependence of  $T\sigma_{\text{pol}}L$  for various frequencies and temperatures. The solid lines denote the quadratic concentration dependence [Eq. (43)] and the dashed lines are drawn to connect points of one temperature when necessary for clarity.

<sup>21</sup> *AC Capacitance, Dielectric Constant, and Loss Characteristics of Electrical Insulating Materials*, D 150-54T (ASTM Standards on Electrical Insulating Materials, American Society for Testing Materials, Philadelphia, Pennsylvania, 1954), p. 103.

the bridge's dissipation factor capacitor can be ignored. This is valid when  $F/F_0 \leq 1$ , which applies in our case.

Then  $\sigma_{ac}$  and  $\epsilon_{pol}$  follow the equations

$$\sigma_{ac} = Gg, \quad (46)$$

$$\epsilon_{pol} = (C_b - C_0)g/\epsilon_0, \quad (47)$$

where  $\epsilon_0$  is the permittivity of space and  $g$  is the geometry factor.  $C_0$  is the circuit capacitance in parallel with the sample plus the lattice capacitance of the sample.  $C_b$  was estimated from the Kramers-Kronig relations using the second of two procedures outlined by PG.<sup>5</sup>

#### APPENDIX B

We now calculate the probability  $H(\Delta, r)$  that a singly ionized acceptor pair of size  $r$  has an energy difference  $\Delta$  between its members. The assumptions are: (1) The nearest acceptor to each donor is ionized by that donor and forms one member of an active (singly ionized) pair; (2) the energy  $\Delta$  of the pair is caused only by the donor which ionized it.

Consider a donor  $D$  and two acceptors  $A$  and  $A_1$  as shown in Fig. 12. Let  $A$  be the nearest acceptor to  $D$ . The distance between  $A$  and  $A_1$  is defined to be  $r$ .  $A_1$  may be anywhere on the sphere of radius  $r$  outside the sphere of radius  $R$ .  $H(\Delta, r)$  is the probability that  $\Delta$  is the energy difference between  $A$  and  $A_1$ .

$$\begin{aligned} \Delta &= (e^2/\epsilon_{Ge})[R^{-1} - R_1^{-1}] \\ &= (e^2/\epsilon_{Ge})[R^{-1} - (R^2 + r^2 + 2Rr \cos\theta)^{-1/2}]. \end{aligned} \quad (48)$$

For fixed  $\Delta$  there is a maximum and a minimum value of  $R$  which will satisfy Eq. (48) corresponding to  $\theta=0$  and  $\pi$ , respectively. (This should be clear from the geometry of the problem.) They are given by

$$\begin{aligned} R_{\max} &= \frac{1}{2}[r^2 + 4e^2r/\epsilon_{Ge}\Delta]^{1/2} - \frac{1}{2}r, \\ R_{\min} &= \frac{1}{2}r + e^2/\epsilon_{Ge}\Delta - \frac{1}{2}[r^2 + (2e^2/\epsilon_{Ge}\Delta)^2]^{1/2}. \end{aligned} \quad (49)$$

For fixed  $R$ , there is a range of  $\Delta$  corresponding to a range of  $\theta$ . There is a maximum value of  $\theta$ ,  $\theta_{\max}$ ,

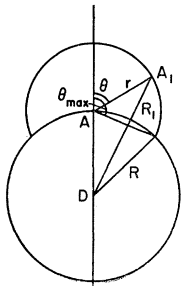


FIG. 12. Diagram used in calculation of  $H(\Delta, r)$ . See text.

corresponding to  $R=R_1$ . It is given by  $-\cos\theta_{\max} = r/2R$  when  $r/2R \leq 1$ . However, if  $r/2R > 1$ , then  $\theta_{\max} = \pi$ . Both cases are represented by the expression

$$-\cos\theta_{\max} = \min(1, r/2R); \quad (50)$$

i.e.,  $-\cos\theta_{\max}$  is 1 or  $r/2R$ , whichever is less.

For fixed  $R$ , the probability that the energy of the pair will be  $\Delta$  is

$$P(\Delta, R)d\Delta = -P_1(\theta)d\theta = -\sin\theta d\theta / \int_0^{\theta_{\max}} \sin\theta d\theta. \quad (51)$$

(The minus sign accounts for the fact that  $d\theta/d\Delta < 0$ .) By solving Eq. (48) for  $\cos\theta$  and taking differentials, one finds

$$-\sin\theta d\theta = R^2\epsilon_{Ge}(re^2)^{-1}(1 - R\epsilon_{Ge}\Delta/e^2)^{-3}d\Delta. \quad (52)$$

Using Eqs. (52) and (50), Eq. (51) becomes

$$P(\Delta, R) = R^2\epsilon_{Ge}[re^2(1 - R\epsilon_{Ge}\Delta/e^2)^3 \times \min(2, 1 + r/2R)]^{-1}. \quad (53)$$

$R$ , of course, is not fixed. The probability of  $R$  occurring is given by the Poisson formula

$$P_2(R)dR = 3R^2R_A^{-3}dR \exp[-(R/R_A)^3], \quad (54)$$

where  $R_A = (\frac{4}{3}\pi N_A)^{-1/3}$  is the average distance between acceptors. Then the desired probability is

$$H(\Delta, r) = \int_{R_{\min}}^{R_{\max}} P_2(R)P(\Delta, R)dR. \quad (55)$$

We introduce the parameters

$$\Delta_0 = e^2r/\epsilon_{Ge}R_A^2, \quad (56)$$

$$\gamma = r/R_A, \quad (57)$$

$$x = R/R_A. \quad (58)$$

Using Eqs. (49), (53)–(58), we get out final expression

$$\begin{aligned} \Delta_0 H(\Delta, r) &= 3 \int_{x_{\min}}^{x_{\max}} \frac{x^4 \exp(-x^3) dx}{(1 - \gamma x \Delta / \Delta_0)^3 \min(2, 1 + \gamma/2x)}, \end{aligned} \quad (59)$$

where

$$\begin{aligned} x_{\max} &= \frac{1}{2}[\gamma^2 + 4\Delta_0/\Delta]^{1/2} - \frac{1}{2}\gamma, \\ x_{\min} &= \frac{1}{2}\gamma + \Delta_0/\gamma\Delta - \frac{1}{2}[\gamma^2 + (2\Delta_0/\gamma\Delta)^2]^{1/2}. \end{aligned} \quad (60)$$

The integrand does not contain a singularity since  $\gamma x_{\max}\Delta/\Delta_0 < 1$ .

The integral was evaluated numerically and the results are shown in Fig. 8.